Il Quaternario
Italian Journal of Quaternary Sciences
***22**(1), 2009 - 109-116*

STRAIN RATE FIELD FROM GEODETIC VELOCITY MEASUREMENTS: AN APPROACH BASED ON NUMERICAL MODELLING

Viti M.[1], Mantovani E.[1], Cenni N.[2], Babbucci D.[1]
[1]Dip. di Scienze Della Terra, Univ. di Siena, e-mail: vitimar@unisi.it
[2]Dip. di Fisica, Univ. di Bologna

ABSTRACT: M. Viti *et al*., *Strain rate field from geodetic velocity measurements: an approach based on numerical modelling*. (ISSN IT 0394-3356, 2009).
The reconstruction of the strain rate field from geodetic velocity data is often carried out by geometrical procedures, such as subdivision in polygons of the geodetic network or interpolation of the velocity vectors. However, as discussed in this work, this kind of approach presents several shortcomings, which may affect the reliability of the computed strain rate field. In particular, the results of such approaches may be strongly biased by the fact that the mechanical properties of the crust in the zone considered are neglected. This problem may be overcome by the use of numerical modelling imposing the geodetic velocity vectors as kinematic constraints. As an example, the proposed procedure is applied to the Central Mediterranean region to determine the strain rate field associated with a recent geodetic (GPS) velocity data set available in literature. The comparison of the result so obtained with the one derived by polygon subdivision shows that numerical modelling allows a more detailed and reliable recognition of the strain-rate field in the zones involved.

RIASSUNTO: M. Viti et al*.,* Calcolo del campo di deformazione da velocità geodetiche: metodologia basata sulla modellazione numerica*. (ISSN IT 0394-3356, 2009).*
Il calcolo del campo di deformazione associato ad una rete di velocità geodetiche è spesso effettuato mediante procedure di tipo geometrico, come la suddivisione in poligoni della rete geodetica o l'interpolazione di velocità. In questo lavoro viene messo in evidenza che tali procedure presentano importanti limitazioni che potrebbero inficiare l'attendibilità dei risultati ottenuti. Il problema principale è che gli approcci di tipo geometrico non impongono che la deformazione calcolata sia compatibile con le proprietà meccaniche della crosta. Questo problema può essere superato adottando una procedura alternativa, basata sulla modellazione numerica della zona considerata. Il modello è costituito da una piastra elastica sottile, la cui deformazione è vincolata dalle velocità geodetiche. Come esempio, l'approccio proposto è applicato alla zona mediterranea centrale per calcolare il campo di deformazione associato ad una recente soluzione GPS disponibile in letteratura. Il confronto tra i risultati ottenuti ed il campo di deformazione calcolato mediante suddivisione in poligoni mostra che la modellazione numerica permette una più dettagliata e realistica definizione della distribuzione spaziale del tasso di deformazione nella regione considerata.

Key words: Crustal Strain Rate, GPS, Numerical modelling, Central Mediterranean.

Parole chiave: Campo della deformazione crostale, GPS, Modellazione numerica, Mediterraneo Centrale.

INTRODUCTION

It is largely recognized that the reconstruction of the present strain field in a tectonic zone may provide major constraints for the elaboration of geodynamic and seismotectonic models (e.g., Mantovani *et al*., 2001; Viti *et al*., 2004) and for seismic hazard assessment (e.g., Bird & Liu, 2007). Until recent years, such information was derived from the analysis of neotectonic and seismological data. However, difficulties in fault sampling and dating may severely limit the use of field kinematic indicators (e.g., Marrett & Allmendinger, 1990) and incompleteness and shortness of seismicity catalogues, along with uncertainties in source mechanism of historical earthquakes, may considerably bias the strain regimes obtained from moment tensor summation (e.g., Viti *et al*., 2001).

Due to the rapid development of reliable and relatively inexpensive space geodetic techniques, in particular the Global Positioning System (GPS), a new important approach for crustal deformation studies is now available (e.g. Altamimi *et al*., 2007). So far, the computation of the strain rate field associated with velocity data is often carried out by geometrical approaches. The two most popular procedures are synthetized in the following:

1) Polygonal subdivision: the study area is subdivided in a complex of polygons with vertexes in the GPS stations and the average strain rate tensor is computed in each polygon (e.g. Feigl *et al*., 1990; Lamb, 2000; Serpelloni *et al*, 2005);
2) Interpolation: a continuous velocity field is determined by interpolating geodetic velocities, after which then the related strain rate field is derived (e.g. Wessel & Bercovici, 1998; Beavan & Haines, 2001; Caporali *et al*., 2003).

However, both these approaches present major limitations which may lead to unreliable strain rate fields. The main shortcoming is that they do not take into account the fact that the deformation of a real medium is not free, being controlled by continuum mechanics and rock properties. Other problems are related to the fact that in each polygon, considered in the first technique, the strain rate tensor computed for the barycenter is assumed to be homogeneous throughout the polygonal area, despite the fact that this con-

dition is rather unlikely in real contexts. On the other hand, when interpolation is considered, the computed strain rate field may be significantly influenced by the technique adopted.

The above problems may be overcome by computing the strain rate field by numerical modelling of real crustal structures under the constraints imposed by geodetic velocities (e.g., LUNDGREN *et al*., 1998). In this work, we apply the above approach to the Central Mediterranean region and compare the results obtained with the ones provided by a polygonal procedure.

STRAIN RATE FIELD RECONSTRUCTION IN THE CENTRAL MEDITERRANEAN

To show an example of the differences that may derive from computing the strain field by numerical modeling or by a polygonal procedure, we have considered the GPS velocity solution obtained for the Central Mediterranean by SERPELLONI *et al*. (2005), using measurements carried out in the period 1991-2002 in a rather uniform density of permanent station (Fig.1).

Numerical modelling

The region covered by the geodetic network is simulated by a thin elastic sheet, using a finite element procedure implemented in the COMSOL Multiphysics software package (COMSOL™, 2005). The sheet (about 1.500 x 1500 km^2) has been discretized by a finite element grid including 4612 triangular quadratic Lagrange elements. Uniform elastic properties have been assigned to the whole sheet (Young modulus E = 7.10^{10} Pa and Poisson ratio ν = 0.25 after LUNDGREN *et al*., 1998).

Velocity vectors have been imposed to the nodes of the grid, corresponding to station sites. In the model, velocities are applied as instantaneous displacements. Plane stress conditions have been adopted, as usually done in thin sheet approximation involving horizontal loading (e.g., SEGEL, 1987).

A series of numerical experiments, aimed at exploring the role of the internal and boundary conditions imposed on the elastic sheet, suggests that the solution of the elastic problem (i.e. the velocity and strain rate fields) is mostly controlled by the internal kinematic constraints (velocities imposed to the station sites). Since a change of boundary conditions only (moderately) affects the peripheral zones of the model we show the solution obtained by imposing the most simple boundary condition, that is null stress on the four sides of the sheet (Fig.2).

The principal axes of the computed horizontal strain rate tensor show large lateral variations in both orientation and magnitude, ranging from negligible values to tens of nanostrain yr^{-1} (1 nanostrain yr^{-1} = 3.17 10^{-17} s^{-1}). The largest strain rates occur in the eastern part of the model (western Greece, among the ORID, IGOU and KARI stations. High strain rate values, associated to NE-SW lengthening, also occur at the boundary between Central and Southern Apennines, near

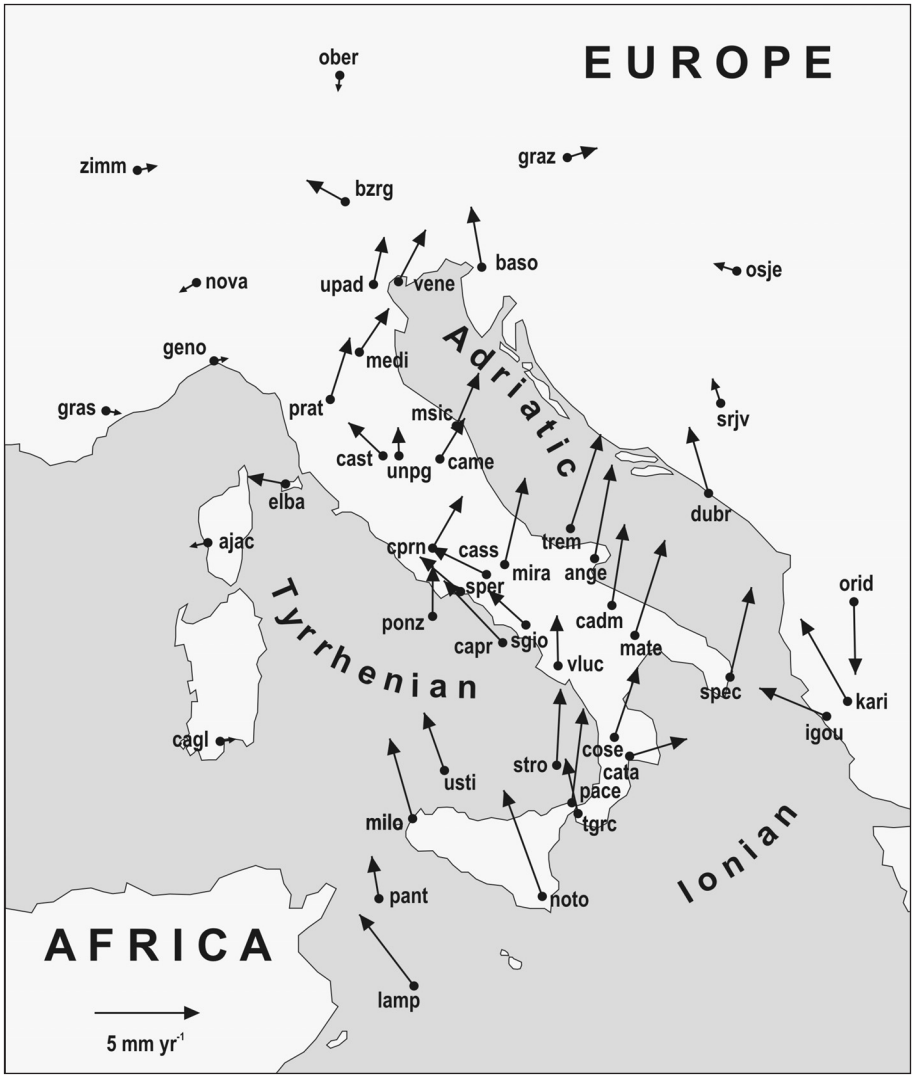

Fig. 1 - GPS velocity solution for the Central Mediterranean proposed by SERPELLONI *et al*. (2005). Arrows indicate the residual horizontal velocities with respect to an European reference frame (absolute Euler pole located at latitude φ = 53.8 ± 1.9 °N, longitude λ = -105.5 ± 0.9 °E with angular velocity ω = 0.249 ± 0.003 ° Myr^{-1}). Abbreviations of permanent GPS stations as in SERPELLONI *et al*. (2005).

Velocità GPS per il Mediterraneo centrale proposte da SERPELLONI et al. (2005). *Le frecce rappresentano le velocità orizzontali residue calcolate rispetto ad un sistema di riferimento europeo, con polo euleriano assoluto: lat φ = 53.8 ± 1.9 °N , long λ = -105.5 ± 0.9 °E, velocità angolare ω = 0.249 ± 0.003 ° Myr^{-1}. Sigle delle stazioni GPS permanenti come in* SERPELLONI et al. *(2005).*

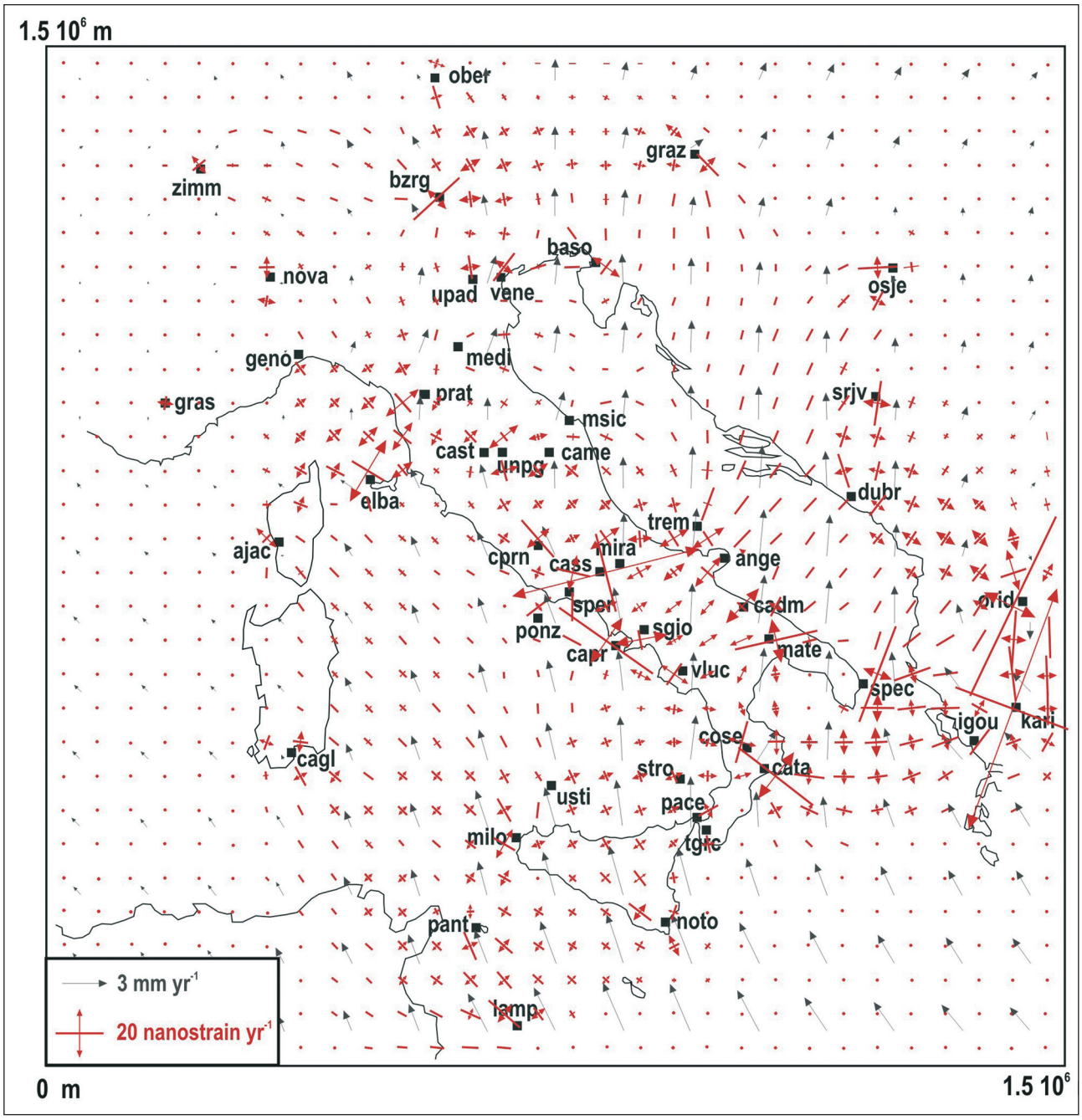

Fig. 2 - Strain rate field (red bars and arrows) obtained by the finite element modelling described in the text. Computed velocity vectors (gray arrows) are reported on a 15 x 15 point grid (100 km spacing). Principal axes of the strain rate tensor are reported on a 30 x 30 point grid (50 km spacing). The velocity vectors (Fig. 1) have been imposed in station sites. The null stress condition has been imposed to the boundaries of the model. A Young modulus (E) of 7 10^{10} Pa and a Poisson ratio (ν) of 0.25 have been adopted.

Campi della velocità e del campo di deformazione ottenuti dalla modellazione agli elementi finiti descritta nel testo. I vettori di velocità (frecce grigie) sono riportati su una griglia con spaziatura di 100 km tra punti adiacenti. Gli assi principali del tensore del tasso di deformazione sono riportati (in rosso) su una griglia con spaziatura di 50 km. I vettori velocità mostrati in figura 1 sono stati applicati nei punti del modello corrispondenti alle stazioni GPS. La condizione di sforzo nullo è stata imposta ai bordi del modello. I parametri elastici adottati per la piastra sono E = 7 10^{10} Pa e ν = 0.25.

the CASS and MIRA stations. Significant transtensional strain rates occur in the Tuscany-Umbria zone, among the ELBA, PRAT, UNPG and CAST stations. Compressional to transpressional strain characterizes the northern and northeastern sectors of the model (Southern Alps and Dinarides).

Comparison with the strain rate field derived by a polygonal procedure

The strain rate field given by Serpelloni *et al*. (2005) is shown in figure 3. The region covered by the geodetic network has been subdivided in 37 polygons, with vertexes in the station sites. The horizontal strain

rate tensor is computed in the barycenter of each polygon by using the vectors in the respective vertexes (Feigl *et al*., 1990). A comparison of figure 3 with the strain rate field shown in figure 2 clearly shows that the procedure here proposed allows us to recognize the lateral heterogeneities of the strain rate pattern inside the geodetic network. This would also be allowed by interpolation of geodetic vectors, but such procedure does not guarantee that the results obtained are compatible with rock mechanics. One must be aware that the reliability of the results provided by numerical modelling depends on how the adopted rheological properties are representative of the real context. On the other hand, the results of this last approach are certainly more realistic than the average strain rate provided by geometrical procedures or than the strain pattern obtained by allowing a free deformation of the crust in the zone involved. To better focus on this crucial aspect, details on the numerical and geometrical strain rate tensors are provided (Figs 4, 5 and 6) for three polygons (33, 14 and 4 in figure 3).

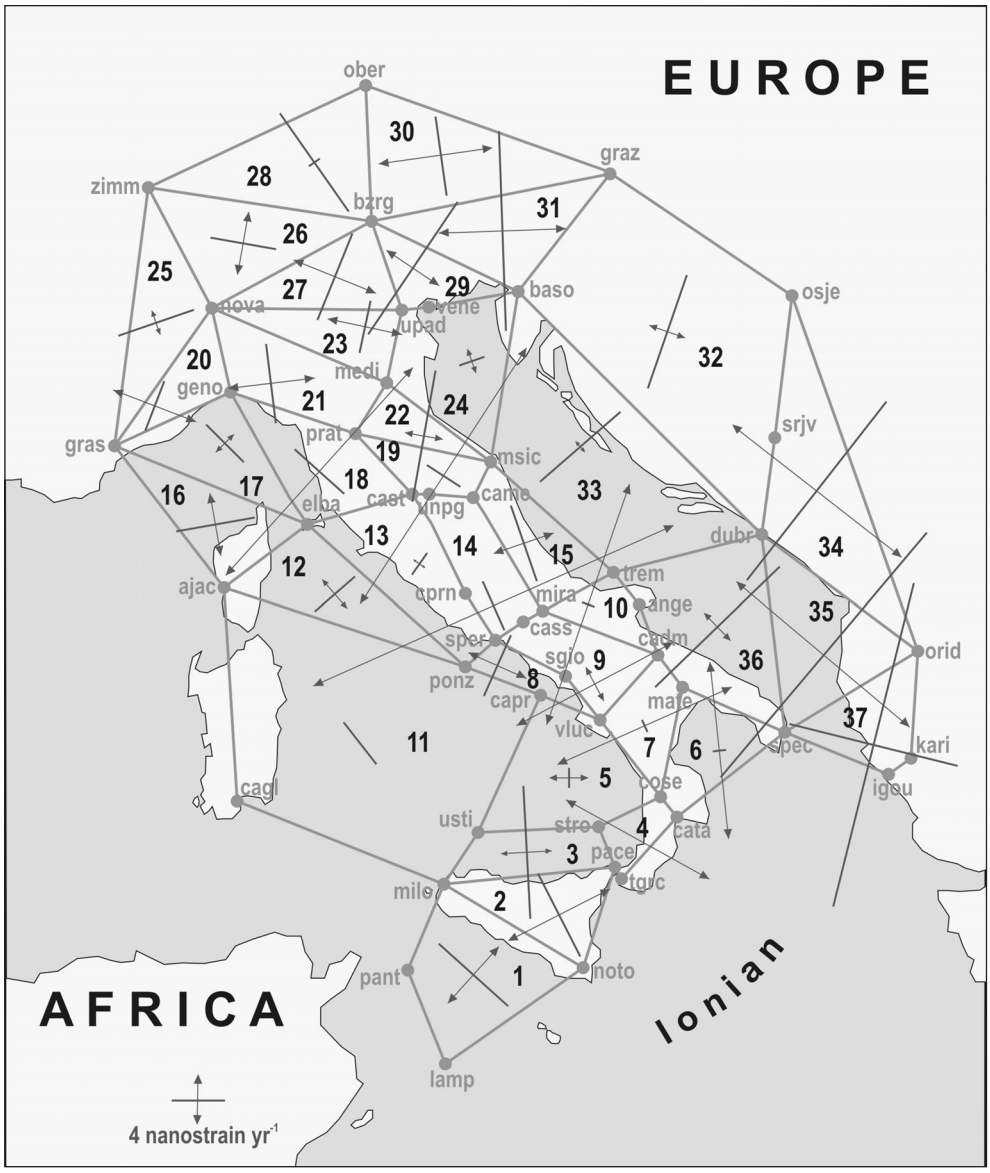

Fig. 3 - Strain rate field obtained by subdiving the region considered in 37 polygons (after Serpelloni *et al*., 2005). For each polygon, the principal axes of the horizontal strain rate tensor, computed in the polygon barycentre, are shown.

Campo del tasso di deformazione ottenuto mediante suddivisione della rete geodetica in 37 poligoni (da Serpelloni et al*., 2005). Gli assi principali del tensore del tasso della deformazione orizzontale sono calcolati nel baricentro di ogni poligono.*

In polygon 33, covering the central-northern Adriatic region (Fig. 4), the geometrical approach provides a roughly NE-SW uniform shortening, which is not compatible with the results of neotectonic and seismological data that indicate a roughly SW-NE compression at the eastern Adriatic border and a rather heterogeneous strain field in the Apennine belt, involving shortening at the outer fronts of the chain and extensional to transtensional strain regime in the axial part (e.g., Cello *et al*., 2003; Piccardi *et al*., 2006; Ferranti *et al*., 2008, 2009). This last evidence is more compatible with the results of numerical modelling for the above polygon, which shows that the direction of maximum shortening considerably changes from the western sector (where it is about E-W near the stations of MSIC and BASO) to the eastern part (roughly N-S near station TREM and NNE-SSW to NE-SW between stations BASO and DUBR).

In polygon 14, covering the axial part of the Central Apennines (Fig. 5), the polygonal solution provides a roughly E-W uniform extensional style, that does not report any evidence of the sinistral transtensional regime recognized in that zone by the analysis of neotectonic and seismicity data (e.g., Amoruso *et al*., 1998; Galadini, 1999; Piccardi *et al*., 2006). In the same polygon, the numerical solution shows a dominant strike-slip strain rate field with significant lateral variations of the amplitude and ratio of principal axes, which is more consistent with the observed strain pattern.

In polygon 4, located in the northern part of Southern Calabria (Fig. 6), the polygonal solution shows a uniform NW-SE extension, that does not inform us about the considerably heterogeneous strain pattern

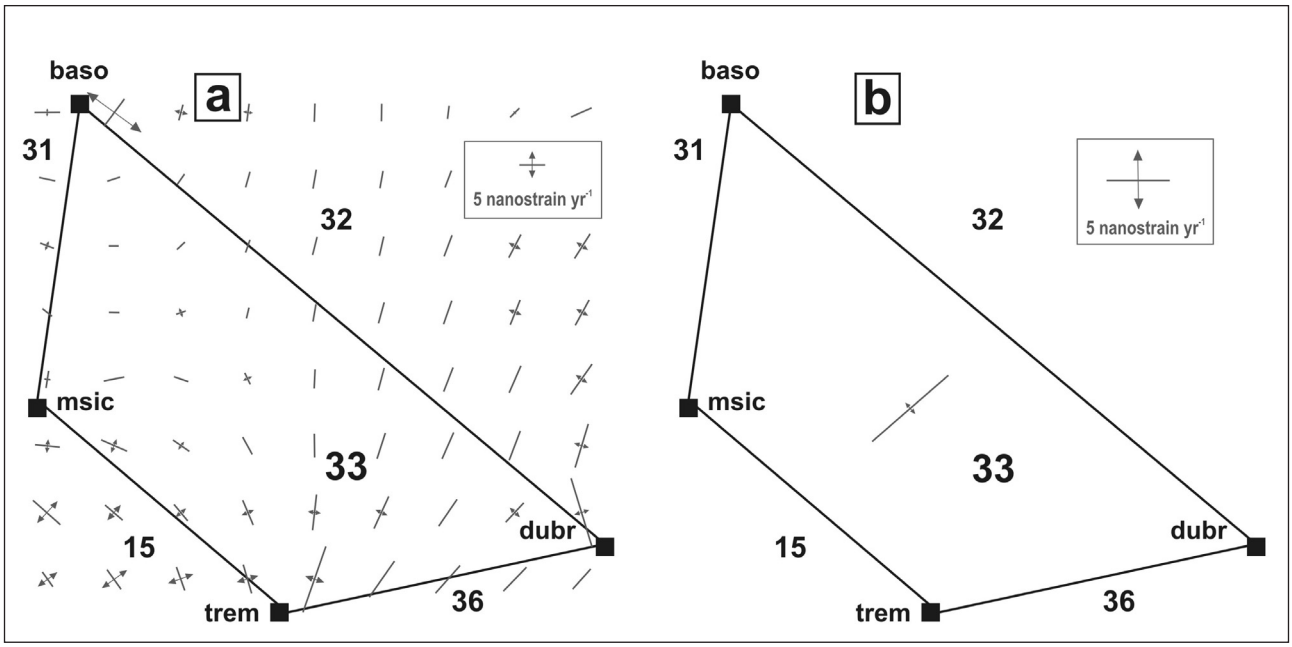

Fig. 4 - Strain rate field for the polygon 33 of figure 3 (Central Adriatic). Station abbreviations as in figure 1. **a)** Strain rate field provided by the numerical solution shown in figure 2. Grid spacing is 50 km. **b)** Strain rate computed in the barycenter (after SERPELLONI *et al*., 2005).

Campo del tasso di deformazione per il poligono 33 di figura 3 (Adriatico centrale). Le sigle delle stazioni GPS sono quelle indicate in figura 1. ***a)*** *Campo del tasso di deformazione relativo alla soluzione numerica di figura 2. La spaziatura dei punti della griglia è 50 km.* ***b)*** *Campo del tasso di deformazione calcolato nel baricentro (da* SERPELLONI et al., *2005).*

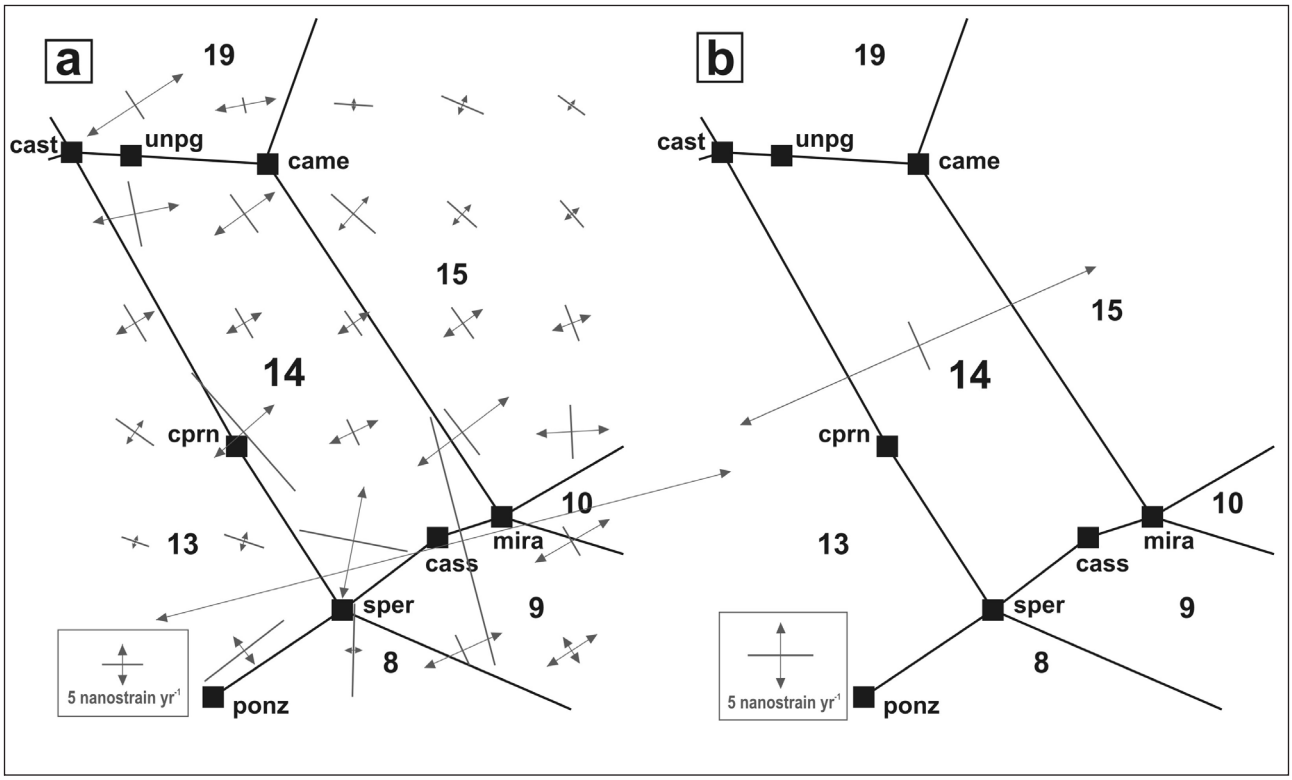

Fig. 5 - Strain rate field for the polygon 14 of figure 3 (Central-Northern Apennines). Station abbreviations as in figure 3. **a)** Strain rate field provided by the numerical solution shown in figure 2. Grid spacing is 50 km. **b)** Strain rate computed in the barycenter (after SERPELLONI *et al*., 2005).

Campo del tasso di deformazione per il poligono 14 di figura 3 (Appennino centro-settentrionale). Le sigle delle stazioni GPS sono quelle indicate in figura 1. ***a)*** *Campo del tasso di deformazione relativo alla soluzione numerica di figura 2. La spaziatura dei punti della griglia è 50 km.* ***b)*** *Campo del tasso di deformazione calcolato nel baricentro (da* SERPELLONI et al., *2005).*

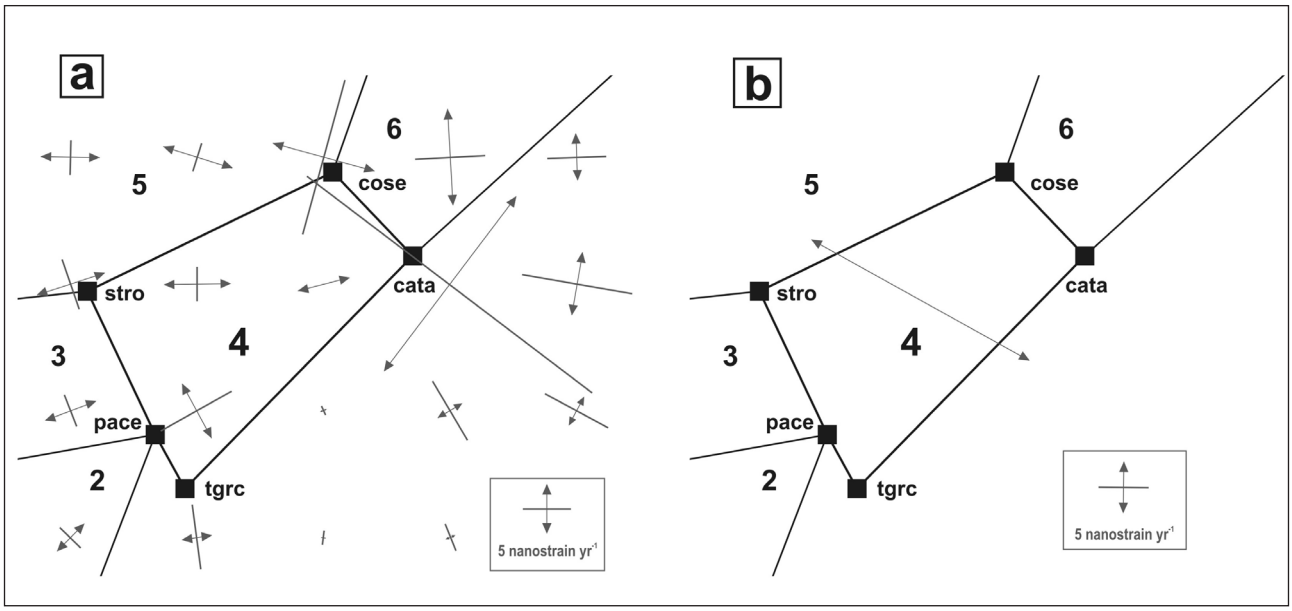

Fig. 6 - Strain rate field for the polygon 4 of figure 3 (Southern Calabria). GPS station abbreviations as in figure 1a. **a)** Strain rate field provided by the numerical solution shown in figure 2. Grid spacing is 50 km. **b)** Strain rate computed in the barycenter (After SERPELLONI *et al*., 2005).

Campo del tasso di deformazione per il poligono 4 di figura 3 (Calabria meridionale). Le sigle delle stazioni GPS sono quelle indicate in figura 1. ***a)*** *Campo del tasso di deformazione relativo alla soluzione numerica di figura 2. La spaziatura dei punti della griglia è 50 km.* ***b)*** *Campo del tasso di deformazione calcolato nel baricentro (da SERPELLONI* et al., *2005).*

indicated by neotectonic and seismological data (NERI *et al*., 2005, TANSI *et al*., 2007) the analysis of other geodetic information (FERRANTI *et al*., 2008) and the results of seismic surveys (FINETTI, 2005). In the same polygon, the numerical solution indicates a gradual transition from transpression in the southern part to extension in the northern part, which agrees with the results recently obtained by the analysis of geodetic campaignes in that zone (FERRANTI *et al*., 2008).

CONCLUSIONS

Geodetic observations give a precious opportunity to know the present velocity and strain rate field in a region covered by a relatively dense network of stations. However, the computation of the strain rate field associated to the observed velocity vectors must be carried out by a procedure compatible with rock mechanics, which can be achieved, for instance, by numerical simulation with realistic models. In order to provide an example of the differences that can derive from the adoption of the above alternative procedures, we compare the results obtained by their application to a velocity data set in the Central Mediterranean region. Such analysis suggests that numerical modelling allows a more detailed and reliable recognition of the strain-rate field in the zones involved.

REFERENCES

ALTAMIMI Z., COLLILIEUX X., LEGRAND J., GARAYT B. & C. BOUCHER (2007) - ITRF2005: *A new release of the International Terrestrial Reference Frame based on time series of station positions and Earth Orientation Parameters*. J. Geophys. Res., **112**, B09401.

AMORUSO A, CRESCENTINI L & SCARPA R. (1998) - *Inversion of source parameters from near- and far field observations: an application to the 1915 Fucino earthquake, central Apennines, Italy*. J. Geophys. Res, **103**, 29989-29999.

BEAVAN J. & HAINES J. (2001) - *Contemporary horizontal velocity and strain rate fields of the Pacific-Australian plate boundary zone through New Zealand*. J. Geophys. Res., **106**, 741-770.

BIRD P. & LIU Z. (2007) - *Seismic Hazard Inferred from Tectonics: California.* Seismological Research Letters, **78**, 37-48.

CAPORALI A., MARTIN S. & MASSIRONI M. (2003) - *Average strain rate in the Italian crust inferred from a permanent GPS network-II*. Strain rate versus seismic and structural geology. Geophys. J. Int., **155**, 254-268.

CELLO G., TONDI E., MICARELLI L. & MATTIONI L. (2003) - *Active tectonics and earthquake sources in the epicentral area of the 1857 Basilicata earthquake (southern Italy)*. J. Geodynamics, **36**, 37-50.

COMSOL™ (2005) - COMSOL *Multiphysics User's Guide, Version 3.2*. COMSOL AB, Stockholm, 622 pp (www.comsol.com).

FEIGL K.L., KING R.W. & JORDAN T.H. (1990) - *Geodetic measurement of tectonic deformation in the Santa Maria Fold and Thrust Belt, California*. J. Geophys. Res., **90**, 2679-2699.

FERRANTI L., OLDOW J. S., D'ARGENIO B., CATALANO R., LEWIS D., MARSELLA E., AVELLONE G., MASCHIO L., PAPPONE G., PEPE F.& SULLI A. (2008) - *Active deformation in Southern Italy, Sicily and southern*

Sardinia from GPS velocities of the Peri-Tyrrhenian Geodetic Array (PTGA). Boll. Soc. Geol.It. (Ital.J.Geosci.), **127**, 299-316.

Ferranti L., Santoro E., Mazzella M.E., Monaco C. & Morelli D. (2009) - *Active transpression in the northern Calabria Apennines, southern Italy.* Tectonophysics, in press, doi:10.106/j.tecto.2008.11.010.

Finetti I.R. (2005) - *The Calabrian Arc and Subducting Ionian Slab from New CROP Seismic Data*. In: Finetti, I.R. (Ed.), Deep Seismic Exploration of the Central Mediterranean and Italy, CROP PROJECT, Elsevier, **17**, 393-412.

Galadini F. (1999) - *Pleistocene change in the central Apennine fault kinematics, a key to decipher active tectonics in central Italy*. Tectonics, **18**, 877-894.

Lamb S. (2000) - *Active deformation in the Bolivian Andes, South America.* J. Geophys. Res., **105**, 25627-25653.

Lundgren P., Giardini D. & Russo R.M. (1998) - *A geodynamic framework for eastern Mediterranean kinematics*. Geophys. Res. Lett., **25**, 4007-4010.

Marrett R. & Allmendinger R.W. (1990) - *Kinematic analysis of fault slip data*. J. Struct. Geol., **12**, 973-986.

Mantovani E., Cenni N., Albarello D., Viti M., Babbucci D., Tamburelli C. & D'Onza F. (2001) - *Numerical simulation of the observed strain field in the central-eastern Mediterranean region*. J. Geodynamics, **31**, 519-556.

Neri G., Barberi G., Oliva G. & Orecchio B. (2005) - *Spatial variations of seismogenic stress orientations in Sicily, south Italy*. Phys. Earth Planet. Int., **148**, 175-191.

Piccardi L., Tondi G. & Cello G. (2006) - *Geo-structural evidence for active oblique extension in South-Central Italy*. In: Pinter, N. et al. (Eds.), The Adria microplate: GPS Geodesy, Tectonics and Hazard, Springer, 95-108.

Segel L.A. (1987) - *Mathematics applied to continuum mechanics*. Dover Publications, New York, 590 pp.

Serpelloni E., Anzidei M., Baldi P., Casula G. & Galvani A. (2005) - *Crustal velocity and strain-rate fields in Italy and surrounding regions: new results from the analysis of permanent and non-permanent GPS networks*. Geophys. J. Int., **161**, 861-880, doi:10.1111/j.1365246X.2005.02618.x.

Tansi C., Muto F., Critelli S. & Iovine G. (2007) - *Neogene-Quaternary strike-slip tectonics in the central Calabrian Arc (southern Italy)*. J. Geodynamics, **43**, 393-414.

Viti M., Albarello D. & Mantovani E. (2001) - *Classification of seismic strain estimates in the Mediterranean region from a 'bootstrap' approach.* Geophys. J. Int., **146**, 399-415.

Viti M., De Luca J., Babbucci D., Mantovani E., Albarello D. & D'Onza F. (2004) - *Driving mechanism of tectonic activity in the northern Apennines: quantitative insights from numerical modelling*. Tectonics, **23**, TC4003.

Wessel P. & Bercovici D. (1998) - *Interpolation with splines in tension: a Green's function approach*. Math. Geol., **30**, 77-93.

Ms. ricevuto il 14 ottobre 2008
Testo definitivo ricevuto il 6 aprile 2009

Ms. received: October 14, 2008
Final text received: April 6, 2009